

Introducing tools to test Higgs interactions via WW scattering I: one-loop calculations and renormalization in the HEFT

Domènec Espriu,^{1,*} Federico Mescia,^{1,†} and Iñigo Asiáin^{1,‡}

¹*Departament de Física Quàntica i Astrofísica,*

Institut de Ciències del Cosmos (ICCUB),

Universitat de Barcelona, Martí Franquès 1, 08028 Barcelona, Spain

Effective field theories are useful tools to search for physics beyond the Standard Model (SM). However, effective theories can lead to non-unitary behavior with fastly growing amplitudes. This unphysical behavior may lead to large sensitivity to SM deviations, making necessary a unitarization of the amplitudes prior to a comparison with experiment. In the present work, we focus on all the processes entering two-Higgs production by longitudinal WW scattering: we perform a full one-loop calculation of all relevant processes, we determine the necessary counterterms in the on-shell scheme, and we study how the full inclusion of the gauge degrees of freedom modifies the previously computed masses and widths of the dynamical resonances arising from the unitarization process in the vector-isovector channel. Altogether, we are able to provide the technical tools that are needed to study the low-energy couplings in the Higgs effective theory under the requirements of unitarity and causality.

^{*}Electronic address: espriu@icc.ub.edu

[†]Electronic address: mescia@ub.edu

[‡]Electronic address: iasiain@icc.ub.edu

Contents

I. Introduction	1
II. The effective Lagrangian	3
III. Tree level calculation of the relevant $2 \rightarrow 2$ processes	9
A. $W^+W^- \rightarrow ZZ$	10
B. $W_LW_L \rightarrow hh$	11
C. $hh \rightarrow hh$	11
D. Counterterms	11
E. Auxiliary processes: $h \rightarrow \omega\omega$, $h \rightarrow hh$ and $h \rightarrow W\omega$	12
IV. One loop calculation of the relevant $2 \rightarrow 2$ processes and counterterms	13
A. Real part: The Equivalence Theorem	14
1. $\omega^+\omega^- \rightarrow zz$	15
2. $\omega^+\omega^- \rightarrow hh$	15
3. $hh \rightarrow hh$	16
B. Determination of counterterms	16
C. Cross-checks and comparison with previous results	18
D. Imaginary part: The Optical theorem	20
V. Unitarization	21
A. Amplitudes at high energies	21
B. The Inverse Amplitude Method (IAM)	23
C. Vector resonances	25
D. Checking unitarity	26
E. Influence of the new HEFT constants	27
VI. Conclusions	28
Acknowledgements	30
References	30

I. INTRODUCTION

Since the discovery in 2012 of a light scalar by ATLAS [1] and CMS [2], so far compatible with the Standard Model (SM) Higgs, a lot of questions have arisen regarding the origin of such a scalar and hence the properties of the electroweak symmetry breaking sector (EWSBS) [3–9].

To explore the nature of EWSBS beyond-the-SM (BSM), the scattering of longitudinally polarized electroweak gauge bosons is one of the most sensitive channels. The appearance of heavy resonances in the scattering of longitudinally polarized gauge bosons, for example, will be a clear indication of the existence of a strong dynamics behind EWSB [10–14].

The main properties of these resonances can be studied using effective theory treatment together with partial wave analysis and unitarization techniques [10, 15–20]. Over the years, the use of Inverse Amplitude Method (IAM) to build unitarity amplitudes has been successfully applied to explain the resonances in the pion-pion scattering [21–28]. The IAM allows us to predict mass and width of dynamically generated resonances from the unitarized amplitudes of the low-energy effective theory. In turn, this also allows us to set bounds on the couplings of the underline effective theories. Small deviations of these couplings from the SM values lead to rapidly-increasing cross sections at high energy, and hence large unitarity violations for the IAM amplitudes.

Among the open questions of the EWSBS is the nature of the Higgs potential. Even if one assumes that the Higgs-like scalar found is truly elementary, are its self-interactions the ones predicted by the textbook SM?

Indeed, this is one of the main purposes of future machines such as the future ILC linear collider in Japan or the planned FCC e^+e^- at CERN [29]. In all these cases, setting bounds on effective couplings needs a *bona fide* and fair comparison that requires using unitarized amplitudes when departures from the SM values could be potentially large.

The purpose of this article is to provide some tools that would make this comparison possible. More specifically, we compute the renormalization counterterms at one-loop that are required to calculate the processes $W_L W_L \rightarrow W_L W_L$, $W_L W_L \rightarrow hh$ and $hh \rightarrow hh$. All these amplitudes enter the unitarization of the $I, J = 0, 0$ channel. Moreover, we also provide for these $2 \rightarrow 2$ processes the corresponding renormalized amplitudes. Here, we calculate the

full $\mathcal{O}(g^2)$ contributions of these processes. This paper thus completes the previous work in Refs. [10, 15, 16], where the analysis was carried out in the limit of no gauge interactions, $g = 0$; only the longitudinal parts of the EW bosons, i.e Goldstone bosons (GBs), were taken into account inside the loops. In the present work, as mentioned, we relax that approximation and allow transverse modes to propagate in the process. This also improves a weak point of the previous studies because with the assumption $g = 0$ in [10, 15, 16], authors consistently set $M = 0$ for the real part of the loop calculation. With respect previous works, we also compute the processes involving double Higgs production.

The derivation is made in the framework of the Higgs effective field theory (HEFT) [3–9, 12], where the global symmetries are non-linearly realized and the complex doublet structure of the SM is not assumed a priori (see e.g. the discussions in [30]). The calculation of the $2 \rightarrow 2$ physical amplitudes needed at the one loop level beyond the SM is challenging. Thus, some shortcuts have to be taken in order to have more manageable expressions. The real part of the amplitudes will be computed using the Equivalence Theorem [31–38] (ET), where the longitudinal components of W in the external states are substituted by their Goldstone bosons (GB). This approach is fully consistent in order to study cross-section of longitudinal polarized W at energies much larger of the EW scale. The imaginary part of our amplitude is exactly obtained via the Optical Theorem, where physical W are present in the external legs.

In this work, we make no assumption about the UV strong dynamics so an effective framework will be needed to compute the amplitudes. In our model independent study, the effects of the high energy theory in the low energy regime are encoded in the so called chiral parameters. These couplings in the Lagrangian are absent in the SM and their presence spoil the unitarity of the amplitudes leading them, after unitarization, to exhibit resonances.

For the purposes of this study, the custodial symmetry is assumed to remain exact and the soft breaking of the global symmetry $SU(2)_L \times SU(2)_R$ induced by the gauging of the hypercharge group will be neglected. We believe this approximation to be well justified by the experimental results of the ρ parameter. In this limit, the electromagnetism is removed from the fundamental interactions and the gauge bosons transform exactly as a triplet under the vector (or custodial) subgroup after the global symmetry breaking pattern $SU(2)_L \times SU(2)_R \rightarrow SU(2)_V$, where V stands for $L = R$. The absence of electromagnetic

interactions moves the pole of Z to the very same position of that of the W , making the ρ parameter exactly equal to 1 at every order in perturbation theory.

As mentioned above, a full derivation of the one-loop counterterms in the HEFT, with a dynamical Higgs, is a necessary step in the process. A previous calculation of all the required counterterms does exist in the literature [39, 40]. However, their expressions are not easily translated to the calculation of physical processes, we are interested in. For one thing, the renormalization scheme is not the widely-used on-shell scheme to which we adhere. On the other hand in [39, 40] extensive use is made of the equations of motion and field redefinitions, including some mixing of operators with different chiral dimensions. All this makes their results not directly applicable to a S -matrix calculation. Recently, an independent diagrammatic calculation has been published [41], where a large subset of counterterms are derived (only those involving elastic vector boson scattering). We will review below our agreement with these pre-existing results. It is worthwhile emphasizing that our approach is purely diagrammatic and inspired by the practical requirements needed when S -matrix elements are to be computed.

II. THE EFFECTIVE LAGRANGIAN

The Electroweak Chiral Lagrangian is a non linear gauged effective field theory mimicking chiral perturbation theory, used to investigate low energy QCD, in the electroweak sector [42]. It has been used intensively in the context of effective field theories since the early days of LEP [42–44] in order to put to the test extensions of the SM. In the case of the electroweak sector, it only assumes the local and global properties known to hold at low energies, and makes no specific commitment to the underlying physics. The addition of the Higgs scalar makes this model a Higgs effective field theory (HEFT).

This HEFT contains as dynamical fields, the EW gauge bosons W^\pm, Z, γ ; their associated Goldstone partners $\omega^a = \omega^\pm, z$; and a light Higgs h (the latter could or could not be a Goldstone boson). In the HEFT the goldstones resulting from the electroweak breaking are described by a unitary matrix U that takes values in the coset $SU(2)_L \times SU(2)_R / SU(2)_V$ and the Higgs is a $SU(2)$ singlet. This fact is in contrast to the textbook SM, where the Higgs is part of a complex doublet and transforms alongside the GBs. Effective theories

describing the Higgs as a part of a $SU(2)$ doublet Φ are termed Standard Model effective field theories (SMEFT).

The HEFT is fairly general and its form is largely independent of the details of the EWSBS because it is based only on the symmetry properties and the fact that only the light degrees of freedom are retained. The latter depends on the symmetry breaking pattern $G \rightarrow H$ and the way the electroweak gauge group G_{EW} is embedded in G . In this type of effective theories, the Higgs may or may not be a Goldstone boson. Phenomenologically, having light states other than the Higgs (such as e.g. additional Goldstone bosons) could be worrisome from a phenomenological point of view because it would be very difficult or impossible to find mechanisms that would make them so massive to be able to escape detection. We should then exclude such a possibility from the effective theory.

When can a particular HEFT be written in the form of a SMEFT? Or in other words: when a particular HEFT can be written in terms of the $SU(2)$ doublet Φ ? The answer is the following [45]: given some four-dimensional HEFT scalar manifold with metric $g_{\alpha\beta}(\omega)$ (with $h = \omega^4$), it is possible to find a field reparametrization so that the Lagrangian can be written in terms of the doublet Φ whenever there exists a $SU(2)_L \times SU(2)_R$ invariant point on the coset G/H . This is not always the case, but it happens in the SM.

The non-linearity shows up as momentum dependent vertices with an arbitrary high number of Goldstone boson insertions coming from the expansion of the matrix field

$$U = \exp\left(\frac{i\omega^a\sigma^a}{v}\right) \approx 1 + i\frac{\omega^a\sigma^a}{v} + O\left(\frac{\omega}{v}\right)^2 \quad (1)$$

where $\omega = \{\omega^1, \omega^2, \omega^3\}$ and σ^a represents the $SU(2)$ Pauli matrices. The range of validity of the HEFT itself is given by the parameter controlling the expansion and sets a cut-off for the theory at $\Lambda = 4\pi v \approx 3$ TeV. Given this, we would expect the resonances to emerge at a scale of a few TeV, values in principle reachable at the LHC, but their detection is difficult by several reasons. The main one is that they are produced only in vector boson fusion, a process that is subdominant at the LHC. The fact that the couplings of these putative resonances to the EWSBS are *a priori* unknown is also a serious handicap. In addition, from previous work we know that the dynamical resonances in question are generically narrow and not very visible, particularly if the anomalous couplings do not differ too much from their SM values [10]. However, their appearance is generic and by now their existence in

extensions of the EWSBS seems well established by various unitarization methods [17, 20]. Yet, detailed studies indicate that their confirmation may need the full 3000 fb^{-1} statistics at the LHC [19] if only leptonic decays ($4l$) are considered in the final states and about one order of magnitude less if decays of the vector bosons in two jets are analyzed too ($2j + 2l$) .

The terms of the chiral Lagrangian are organized by the chiral dimension of its local operators. This counts the number of masses and derivatives (momenta) and a piece of the Lagrangian of chiral dimension d , \mathcal{L}_d , will contribute to the process at order $\mathcal{O}(p^d)$. For our analysis with NLO precision, we restrict ourselves to operators up to $\mathcal{O}(p^4)$. The set of operators that participate in $2 \rightarrow 2$ scattering processes and are CP invariant, Lorentz invariant, gauge and custodial symmetric are gathered in the following lagrangians

$$\begin{aligned} \mathcal{L}_2 = & -\frac{1}{2g^2} \text{Tr} \left(\hat{W}_{\mu\nu} \hat{W}^{\mu\nu} \right) - \frac{1}{2g'^2} \text{Tr} \left(\hat{B}_{\mu\nu} \hat{B}^{\mu\nu} \right) + \frac{v^2}{4} \mathcal{F}(h) \text{Tr} \left(D^\mu U^\dagger D_\mu U \right) \\ & + \frac{1}{2} \partial_\mu h \partial^\mu h - V(h) \end{aligned} \quad (2)$$

$$\begin{aligned} \mathcal{L}_4 = & -ia_3 \text{Tr} \left(\hat{W}_{\mu\nu} [V^\mu, V^\nu] \right) + a_4 (\text{Tr} (V_\mu V_\nu))^2 + a_5 (\text{Tr} (V_\mu V^\mu))^2 + \frac{\gamma}{v^4} (\partial_\mu h \partial^\mu h)^2 \\ & + \frac{\delta}{v^2} (\partial_\mu h \partial^\mu h) \text{Tr} (D_\mu U^\dagger D^\mu U) + \frac{\eta}{v^2} (\partial_\mu h \partial_\nu h) \text{Tr} (D^\mu U^\dagger D^\nu U) \\ & + i\chi \text{Tr} \left(\hat{W}_{\mu\nu} V^\mu \right) \partial^\nu \mathcal{G}(h) \end{aligned} \quad (3)$$

with the usual definitions

$$\begin{aligned} U &= \exp \left(\frac{i\omega^a \sigma^a}{v} \right) \in SU(2)_V, \quad V_\mu = D_\mu U^\dagger U, \quad \mathcal{F}(h) = 1 + 2a \left(\frac{h}{v} \right) + b \left(\frac{h}{v} \right)^2 + \dots, \\ D_\mu U &= \partial_\mu U + i\hat{W}_\mu U, \quad \hat{W}_\mu = g \frac{\vec{W}_\mu \cdot \vec{\sigma}}{2}, \quad \hat{W}_{\mu\nu} = \partial_\mu \hat{W}_\nu - \partial_\nu \hat{W}_\mu + i \left[\hat{W}_\mu, \hat{W}_\nu \right], \\ V(h) &= -\frac{1}{2} M_h^2 h^2 - \lambda_3 v h^3 - \frac{\lambda_4}{4} h^4 + \dots, \quad \mathcal{G}(h) = 1 + b_1 \left(\frac{h}{v} \right) + b_2 \left(\frac{h}{v} \right)^2 + \dots \end{aligned} \quad (4)$$

From the last operator in (3), and taking into account the definitions above, we will just need for this study the first term in the expansion of $\partial^\nu \mathcal{G}(h)$, so we define the new coupling $\zeta \equiv b_1 \chi$. In what concerns the Higgs potential $V(h)$, we will parameterize the departures from the SM trilinear and quartic self couplings using the parameters $d_{3,4}$ such that $\lambda_{3,4} = d_{3,4} \lambda$, being λ the only SM Higgs self-interaction $\lambda = M_h^2/(2v^2)$ coupling.

The relevant HEFT for our processes up to NLO is then the sum of \mathcal{L}_2 , \mathcal{L}_4 and the gauge fixing and Faddeev-Popov terms

$$\mathcal{L} = \mathcal{L}_2 + \mathcal{L}_4 + \mathcal{L}_{GF} + \mathcal{L}_{FP} \quad (5)$$

In the custodial limit and using an arbitrary gauge, the last two pieces are built using the following functions

$$\begin{aligned} f_i &= \partial_\mu W_i^\mu - \frac{gv\xi}{2}\omega_i + \dots \quad i = 1, 2, 3 \\ \mathcal{L}_{GF} &= -\frac{1}{2\xi} \left(\sum_{i=1}^3 f_i^2 \right) \quad \mathcal{L}_{FP} = \sum_{a,b=1}^3 c_a^\dagger \frac{\delta f'_a}{\delta \alpha_b} c_b \end{aligned} \quad (6)$$

where f' stands for the $SU(2)_L \times U(1)_Y$ transformation of the function f and α_a the gauge parameters.

We could enrich the HEFT with additional $SU(2)$ singlets $h^1 (= h), h^2, h^3, \dots$ and a term

$$\frac{1}{2} g_{ij} \partial_\mu h^i \partial^\mu h^j - V(h^1, h^2, \dots). \quad (7)$$

This possibility will not be considered here. The interested reader can see [30] for more details.

The explicit gauge transformation is

$$\hat{W}'_\mu = g_L \hat{W}_\mu g_L^\dagger - \frac{1}{g} g_L \partial_\mu g_L^\dagger \quad U' = g_L U \quad (8)$$

with $g_L = \exp(i\vec{\alpha}(x)\vec{\tau}/2)$, $SU(2)$ matrix. The custodial transformation is

$$U' = g U g^\dagger, \quad (9)$$

where g is a constant $SU(2)$ matrix.

The notation we use roughly follows the conventions of [16]. In [4] the reader may find a complete list of operators in the HEFT up to chiral dimension four¹. Only a small subset of those are relevant to us. Even taking this into consideration, the lagrangians (2) and (3) contain a number of free parameters. Not including these already well established by experiments, we have: a and b in the $O(p^2)$ Lagrangian and $a_3, a_4, a_5, \gamma, \delta, \eta$ and ζ in the $O(p^4)$ Lagrangian. In the SM, $a = b = 1$ and the rest are identically zero. In addition, and of particular interest to us, we have λ_3 and λ_4 in the Higgs potential. We expect departures from the SM values at most of order 10^{-3} , possibly less, in all the ‘anomalous’ couplings.

The experimental situation concerning these couplings is as follows. The situation has been

¹ Some operators are redundant [6], once the bosonic basis together with the fermionic one is considered and equations of motion are used.

Couplings	Ref.	Experiments
$0.89 < a < 1.13$	[46]	LHC
$-0.76 < b < 2.56$	[47]	ATLAS
$-3.3\lambda < \lambda_3 < 8.5\lambda$	[48]	CMS
$ a_1 < 0.004$	[49]	LEP (<i>S</i> -parameter)
$-0.06 < a_2 - a_3 < 0.20$	[50]	LEP & LHC
$-0.0061 < a_4 < 0.0063$	[51]	CMS (from $WZ \rightarrow 4l$)
$ a_5 < 0.0008$	[52]	CMS (from $WZ/WW \rightarrow 2l2j$)

TABLE I: Current experimental constraints on bosonic HEFT anomalous couplings at 95% CL.

See the text about the issue to extract the a_4 bound from the CMS analysis of [52].

summarized e.g. in [14]. The experimental bounds for the chiral coupling a have been measured by ATLAS and CMS in the subprocess $h \rightarrow WW$ at 95% C.L. to be $0.89 < a < 1.13$. Also, the first experimental bounds on the chiral parameter b have been set by ATLAS with the subprocess $hh \rightarrow WW$. The result of this analysis, that assumes the absence of new physics resonances, is $-1.02 < b < 2.71$. As we see, there are still large experimental uncertainties regarding the Higgs couplings to vector bosons. These uncertainties affect operators of chiral dimension 2 and are accordingly expected to be the most relevant ones.

The chiral couplings a_4 and a_5 have received a lot of attention in the past because to a large extent they control the appearance of resonances in the vector-isovector and scalar-isoscalar channels, at least in the approximation where the ET is assumed to hold in its most strict version and the propagation of transverse modes is neglected. Using only the 8 TeV data, in 2017 ATLAS[53] set the bounds $-0.024 < a_4 < 0.030$ and $-0.028 < a_5 < 0.033$. More recently, CMS [51] using the 13 TeV data and only $4l$ decays from WZ scattering was able to set the bounds $-0.0061 < a_4 < 0.0063$, $-0.0094 < a_5 < 0.0098$, about three times better. In [52], CMS studies $2j + 2l$ decays from both WW and WZ scatterings to set the rather

stringent bound² $|a_5| < 0.0008$.

The smallness of these values justifies, in the range of energies where they have been applied, the use of a simple approach, without unitarization. Yet, small as they are, there is still room for new physics resulting from unitarization. For instance this range still allows for the appearance of vector resonances in the range $1.5 < M_V < 2.5$ TeV, both for $a = 1$ and $a = 0.9$ [19].

As for the coupling a_3 , its range of uncertainty is quite large and its influence on the location and properties of resonances in BSM physics has not been assessed yet as this requires a full computation and subsequent unitarization studies including transverse modes of the vector bosons. This will be presented below.

Concerning the Higgs potential parameters, there are not relevant bounds on λ_4 (i.e. on possible departures from the SM relation $\lambda_4 = \lambda = M_h^2/2v^2$). In what concerns λ_3 , and recalling the parameterization $\lambda_3 = d_3\lambda$, some recent bounds have been obtained by ATLAS [57], $-2.3 < d_3 < 10.3$, combining double and single- Higgs analysis at 95% C.L., and by CMS [48], $-3.3 < d_3 < 8.5$, from the subprocess $HH \rightarrow b\bar{b}\gamma\gamma$. To our knowledge, there are no experimental studies on the $\mathcal{O}(p^4)$ chiral parameter ζ . However, as we stress in our work, this parameter plays a role in the WW -scattering at one-loop.

² CMS does not provide results for a_4 and a_5 directly as the analysis relies on the SMEFT, where the Higgs is treated as a doublet and the operators contributing to the scattering of four W are of dimension 8 (unlike in the HEFT where they are of dimension 4). The basis adopted is the one introduced in [54], namely $f_{S,0}/\Lambda^4$ and $f_{S,1}/\Lambda^4$. However, as was later noted in [55, 56], a third operator containing four derivatives of the Higgs doublet, with coefficient $f_{S,2}/\Lambda^4$, exists in the SMEFT and cannot be in general missed. In order to get $f_{S,0}/\Lambda^4$, $f_{S,1}/\Lambda^4$ and $f_{S,2}/\Lambda^4$ one needs to measure WW and WZ final states. This was done in the $4l$ analysis of CMS [51]. However in [52] WW and WZ are combined together and it is not possible to extract $f_{S,2}$ and $f_{S,0}$ separately. Note that only the sum of the operators corresponding to $f_{S,0}$ and $f_{S,2}$ is custodially invariant, but neither of them is. The sum matches the chiral operator multiplying a_4 [56] in the HEFT. Therefore, a valid comparison requires assuming $f_{S,0} = f_{S,2}$ and only then

$$a_4 = \frac{v^4}{8} \frac{f_{S,0}}{\Lambda^4} \Big|_{f_{S,2}=f_{S,0}}.$$

On the other hand, $f_{S,1}$ is custodially invariant and

$$a_5 = \frac{v^4}{16} \frac{f_{S,1}}{\Lambda^4}.$$

III. TREE LEVEL CALCULATION OF THE RELEVANT $2 \rightarrow 2$ PROCESSES

As mentioned in the introduction in order to implement a fair comparison with experiment, we are interested in obtaining unitary amplitudes for the following $2 \rightarrow 2$ processes with one loop precision: $W_L W_L \rightarrow W_L W_L$, $W_L W_L \rightarrow hh$ and $hh \rightarrow hh$. In the first case, the $I = 0, J = 0$ (weak) isospin and angular momentum projection will be most interest to us, but we will actually provide results that can be used for any I, J projection thanks to the relations resulting from the exact isospin symmetry present for $g' = 0$. For instance, provided that custodial symmetry remains exact, from the $W^+ W^- \rightarrow ZZ$ amplitude it is possible to obtain all the remaining $W_L^a W_L^b \rightarrow W_L^c W_L^d$ ones thanks to the isospin relations (see e.g. [10] for details). From Bose and crossing symmetries,

$$\mathcal{A}^{abcd} = \delta^{ab}\delta^{cd}\mathcal{A}(p^a, p^b, p^c, p^d) + \delta^{ac}\delta^{bd}\mathcal{A}(p^a, -p^c, -p^b, p^d) + \delta^{ad}\delta^{bc}\mathcal{A}(p^a, -p^d, p^c, -p^b) \quad (10)$$

that allows us to write

$$\begin{aligned} \mathcal{A}^{+-00} &= \mathcal{A}(p^a, p^b, p^c, p^d) \\ \mathcal{A}^{+-+-} &= \mathcal{A}(p^a, p^b, p^c, p^d) + \mathcal{A}(p^a, -p^c, -p^b, p^d) \\ \mathcal{A}^{+++-} &= \mathcal{A}(p^a, -p^c, -p^b, p^d) + \mathcal{A}(p^a, -p^d, p^c, -p^b) \end{aligned} \quad (11)$$

this means that every amplitude with vector bosons as asymptotic states can be obtained by crossings from the fundamental amplitude $W^+ W^- \rightarrow ZZ$, as mentioned before. Notice that crossing when longitudinally polarized gauge bosons are involved has to be implemented via the momenta and not via Mandelstam variables because the polarization vectors do not transform covariantly (see e.g. the discussion in [10]).

The fixed isospin projections T_I are given by

$$\begin{aligned} T_0 &= 3\mathcal{A}^{+-00} + \mathcal{A}^{+++-} \\ T_1 &= 2\mathcal{A}^{+-+-} - 2\mathcal{A}^{+-00} - \mathcal{A}^{+++-} \\ T_2 &= \mathcal{A}^{+++-} \end{aligned} \quad (12)$$

Taking into account that in this framework the Higgs is a singlet, we can also write the projections for the crossed channels with an $I = 0$ external state and the corresponding isospin amplitudes

$$\mathcal{A}(W_L^a W_L^b \rightarrow hh) = \mathcal{A}^{ab}(p^a, p^b, p_{h,1}, p_{h,2}), \quad T_{Wh,0} = \sqrt{3}\mathcal{A}^{+-}, \quad (13)$$

$$\mathcal{A}(hh \rightarrow hh) = \mathcal{A}(p_{h,1}, p_{h,2}, p_{h,3}, p_{h,4}) = T_{hh,0}, \quad (14)$$

where the last amplitude has obviously only an $I = 0$ projection.

All the tree level amplitudes gathered above have both LO (computed using the Feynman rules from \mathcal{L}_2) and the NLO contributions (obtained using the rules of \mathcal{L}_4).

Below we present the tree level amplitudes for the different $2 \rightarrow 2$ processes that are important for our study. We use the following notation: a superindex indicates the different processes labeled as WW for $W^+W^- \rightarrow ZZ$, Wh for $W^+W^- \rightarrow hh$ and hh for $hh \rightarrow hh$. Also, each amplitude carries a subindices xy that represent a process with a particle y propagating in the x channel. The case with $x = c$ and no y , \mathcal{A}_c , represents the contact interaction of the four external particles. For instance, the amplitude \mathcal{A}_{sh}^{WW} represents a Higgs exchanged in the s-channel of $W^+W^- \rightarrow ZZ$ scattering.

A. $W^+W^- \rightarrow ZZ$

The tree level amplitude includes contribution from the $\mathcal{O}(p^2)$ and $\mathcal{O}(p^4)$ Lagrangian

$$\begin{aligned} \mathcal{A}_c^{WW} = & g^2 \left(((-2a_3 + a_4)g^2 + 1) ((\varepsilon_1 \varepsilon_4)(\varepsilon_2 \varepsilon_3) + (\varepsilon_1 \varepsilon_3)(\varepsilon_2 \varepsilon_4)) \right. \\ & \left. + 2((2a_3 + a_5)g^2 - 1)(\varepsilon_1 \varepsilon_2)(\varepsilon_3 \varepsilon_4) \right) \\ \mathcal{A}_{sh}^{WW} = & -\frac{a^2 g^2 M_W^2 (\varepsilon_1 \varepsilon_2)(\varepsilon_3 \varepsilon_4)}{(p_1 + p_2)^2 - M_H^2} + \frac{a g^4 \zeta}{4((p_1 + p_2)^2 - M_H^2)} [2(\varepsilon_3 \varepsilon_4)((p_1 \varepsilon_2)(p_2 \varepsilon_1) \\ & - (\varepsilon_1 \varepsilon_2)(p_1 + p_2)^2) + 2(\varepsilon_1 \varepsilon_2)(p_3 \varepsilon_4)(p_4 \varepsilon_3)] \\ \mathcal{A}_{tW}^{WW} = & -\frac{(1 - 2a_3 g^2)g^2}{(p_1 - p_3)^2 - M_W^2} [-4((\varepsilon_1 \varepsilon_2)(p_1 \varepsilon_3)(p_2 \varepsilon_4) + (\varepsilon_1 \varepsilon_4)(p_1 \varepsilon_3)(p_4 \varepsilon_2) \\ & + (\varepsilon_2 \varepsilon_3)(p_3 \varepsilon_1)(p_2 \varepsilon_4) + (\varepsilon_3 \varepsilon_4)(p_3 \varepsilon_1)(p_4 \varepsilon_2)) \\ & + 2((\varepsilon_2 \varepsilon_4)((p_1 \varepsilon_3)(p_2 + p_4)\varepsilon_1 + (p_3 \varepsilon_1)(p_2 + p_4)\varepsilon_3) \\ & + (\varepsilon_1 \varepsilon_3)((p_2 \varepsilon_4)(p_1 + p_3)\varepsilon_2 + (p_4 \varepsilon_2)(p_1 + p_3)\varepsilon_4)) \\ & - (\varepsilon_1 \varepsilon_3)(\varepsilon_2 \varepsilon_4)((p_1 + p_3)p_2 + (p_2 + p_4)p_1)] \\ \mathcal{A}_{uW}^{WW} = & \mathcal{A}_{tW}(p_3 \leftrightarrow p_4, \varepsilon_3 \leftrightarrow \varepsilon_4) \end{aligned} \quad (15)$$

where ε_i is the abbreviation for $\varepsilon_L(p_i)$.

B. $W_L W_L \rightarrow hh$

$$\begin{aligned}
\mathcal{A}_c^{Wh} &= \frac{g^2 b}{2} (\varepsilon_1 \varepsilon_2) - \frac{g^2 \eta}{v^2} ((\varepsilon_1 p_4)(\varepsilon_2 p_3) + (p_3 \varepsilon_1)(\varepsilon_2 p_4)) - \frac{2g^2 \delta}{v^2} (p_3 p_4)(\varepsilon_1 \varepsilon_2) \\
&\quad + \frac{g^2 \zeta}{v^2} ((\varepsilon_1 \varepsilon_2)(p_1 + p_2)^2 - 2(p_1 \varepsilon_2)(p_2 \varepsilon_1)) \\
\mathcal{A}_{sh}^{Wh} &= \frac{3g^2 M_h^2}{2((p_1 + p_2)^2 - M_h^2)} \left(a(\varepsilon_1 \varepsilon_2) + \frac{\zeta}{v^2} ((\varepsilon_1 \varepsilon_2)(p_1 + p_2)^2 - 2(p_1 \varepsilon_2)(p_2 \varepsilon_1)) \right) \\
\mathcal{A}_{t\omega}^{Wh} &= \frac{2a^2 g^2 + a\zeta g^4}{2(p_1 - p_3)^2} ((p_3 \varepsilon_1)(p_4 \varepsilon_2)) \\
\mathcal{A}_{tW} &= \frac{a^2 g^2 M_W^2}{((p_1 - p_3)^2 - M_W^2)} \left(\varepsilon_1 \varepsilon_2 + \frac{(p_4 \varepsilon_2)(\varepsilon_1 p_3)}{(p_1 - p_3)^2} \right) + \frac{a g^4 \zeta}{2((p_1 - p_3)^2 - M_W^2)} (2M_h^2(\varepsilon_1 \varepsilon_2) \\
&\quad - (p_4 \varepsilon_2)(p_2 \varepsilon_1) - (\varepsilon_1 p_3)(\varepsilon_2 p_3) + M_W^2 \frac{(p_4 \varepsilon_2)(\varepsilon_1 p_3)}{(p_1 - p_3)^2}) \\
\mathcal{A}_{u\omega}^{Wh} &= \mathcal{A}_{t\omega}^{Wh}(p_3 \leftrightarrow p_4) \\
\mathcal{A}_{uW}^{Wh} &= \mathcal{A}_{tW}^{Wh}(p_3 \leftrightarrow p_4)
\end{aligned} \tag{16}$$

C. $hh \rightarrow hh$

$$\begin{aligned}
\mathcal{A}_c^{hh} &= \frac{8\gamma}{v^4} ((p_1 p_4)(p_2 p_3) + (p_1 p_3)(p_2 p_4) + (p_1 p_2)(p_3 p_4)) - 6\lambda_4 \\
\mathcal{A}_{sh}^{hh} &= - \frac{36\lambda_3^2 v^2}{(p_1 + p_2)^2 - M_h^2} \\
\mathcal{A}_{th}^{hh} &= \mathcal{A}_{sh}^{hh}(p_2 \leftrightarrow -p_3) \\
\mathcal{A}_{uh}^{hh} &= \mathcal{A}_{sh}^{hh}(p_2 \leftrightarrow -p_4)
\end{aligned} \tag{17}$$

D. Counterterms

The divergences eventually appearing in all these processes at the one-loop level have to be absorbed by redefining the parameters appearing at tree level. Namely,

$$\begin{aligned}
v^2 &\rightarrow v^2 + \delta v_{div}^2 + \delta \bar{v}^2, \quad \{h, \omega\} \rightarrow Z_{h,\omega} \{h, W, \omega\}, \quad M_{h,W}^2 \rightarrow M_{h,W}^2 + \delta M_{h,W}^2, \\
\lambda_{3,4} &\rightarrow \lambda_{3,4} + \delta \lambda_{3,4}, \quad a \rightarrow a + \delta a, \quad b \rightarrow b + \delta b, \quad a_i \rightarrow a_i + \delta a_i, \\
\delta &\rightarrow \delta + \delta \delta, \quad \eta \rightarrow \eta + \delta \eta, \quad \gamma \rightarrow \gamma + \delta \gamma, \quad \delta \zeta \rightarrow \delta \zeta + \delta \zeta
\end{aligned} \tag{18}$$

where we recall that $\zeta \equiv \chi b_1$.

Even though the coupling gauge coupling g appears in some of the previous formulae, the relation $M_W = gv/2$ is assumed to all orders and the renormalization of g is fixed by the ones of v and M_W . On the contrary, we cannot assume the SM relation $M_h^2 = 2v^2\lambda$ because this already assumes the persistence of the SM Higgs potential –something that we want to eventually test. It is for this reason too that we keep separate notations λ_3 and λ_4 for the three- and four-point Higgs vertices.

In general all counterterms have both a divergent and a finite part, determined by the renormalization conditions. However, for reasons that will be clear later, we have split the counterterms for v^2 explicitly into divergent and finite pieces.

As we will see in the subsequent, we will determine all counterterms for processes involving only Goldstone bosons, whose calculation is substantially simpler than using vector bosons. This is enough to get all the necessary counterterms. The corresponding tree-level amplitudes for the goldstones will be given in the next section.

E. Auxiliary processes: $h \rightarrow \omega\omega$, $h \rightarrow hh$ and $h \rightarrow W\omega$

In this subsection we collect a series of $1 \rightarrow 2$ tree level processes that are useful to uniquely determine the counterterms. These processes typically cannot take place on-shell, but they have to be rendered finite anyway through the renormalization procedure. They are:

1. $h \rightarrow \omega\omega$ process.

The tree level amplitude of this decay up to NLO is (with p_h the Higgs 4-moment)

$$\mathcal{A}_{tree}^{h \rightarrow \omega\omega} = -\frac{ap_h^2}{v} \quad (19)$$

which leads to the on-shell renormalisation condition

$$\frac{M_h^2}{2v^3} (a\delta v^2 - 2v^2\delta a) + \text{div}(\mathcal{A}_{1-loop}^{h \rightarrow \omega\omega}) = 0 \quad (20)$$

From (19) and with the substitutions that will be specified later, we find the relation between δa and δv^2 , being the counterterms associated to the chiral parameter a and to the vev, respectively.

2. $h \rightarrow hh$ process.

At tree-level, the corresponding amplitude reads

$$\mathcal{A}_{tree}^{h \rightarrow hh} = -6\lambda_3 v. \quad (21)$$

From the cancellation of the divergences of this process at one-loop, we get a relation between $\delta\lambda_3$ and δv^2

$$-\frac{3}{2v^3} (M_h^2 \delta v^2 + 4v^4 \delta\lambda_3) + \text{div}(\mathcal{A}_{1-loop}^{h \rightarrow hh}) = 0 \quad (22)$$

3. $h \rightarrow W\omega$ process

$$\mathcal{A}_{tree}^{h \rightarrow W\omega} = ig \left(a + \frac{M_W^2 \zeta}{v^2} \right) \varepsilon_W p_h. \quad (23)$$

From the cancellation of the divergences of this process at one loop level and with the assumption that the relation $M_W = \frac{1}{2}gv$ is satisfied at every order, we obtain a relation among δv^2 , δM_W^2 , δa and $\delta\zeta$.

$$-i (a M_W^2 \delta v^2 - 2M_W^4 \delta\zeta - av^2 \delta M_W^2 - 2M_W^2 v^2 \delta a) \frac{\varepsilon_W p_h}{M_W v^3} + \text{div}(\mathcal{A}_{1-loop}^{h \rightarrow W\omega}) = 0 \quad (24)$$

IV. ONE LOOP CALCULATION OF THE RELEVANT $2 \rightarrow 2$ PROCESSES AND COUNTERTERMS

In this section we present the one loop calculation of the relevant amplitudes. The amplitudes cannot be expressed in terms of elementary functions as they are given by Passarino-Veltman integrals and they are quite cumbersome. For this reason we just show here the divergent parts (only present in the real part of the amplitude) and the explicit expression for the counterterms.

The calculation of quantum corrections for the processes requires gauge fixing and the inclusion of the Faddeev-Popov ghosts. The results presented below will be given in the Landau gauge $\xi = 0$. Obviously, physical amplitudes should be independent of the gauge choice, but some renormalization constants do depend on the gauge election. In the gauge-fixing processes several differences are present in the HEFT [58, 59] with respect to the textbook SM. On one hand, the Higgs is a singlet so it does not play any role in the symmetry and thus it is not present neither in the gauge fixing piece, nor in the Faddeev-Popov one, i.e, there are no Higgs-ghost interactions. On the other hand, the

gauge condition in (6) translates into ghost-antighost pairs coupled to an arbitrary number of goldstones insertions with a strength depending on the gauge parameter.

As mentioned before, the calculation of the $2 \rightarrow 2$ amplitudes we are interested in is challenging, even at the one loop level. Recall that we will be interested both in the divergent part (to determine counterterms) but also in the much more involved finite part. This is particularly so because there are several free parameters that have to be considered when one moves away from the SM. For this reason it has become customary starting with the work of [10] to split the one-loop calculation into two parts. The imaginary part is computed exactly from the tree-level results described in section III using the Optical Theorem, including only the $\mathcal{O}(p^2)$ pieces. The real part is computed making use of the Equivalence Theorem, replacing the longitudinal vector bosons in the external legs with the corresponding Goldstone bosons. However, the full set of polarizations (including of course transverse modes) will be kept internally inside the loops in the present study.

A. Real part: The Equivalence Theorem

The ET states that at high energies compared to the electroweak scale, the longitudinal projection of the vector boson can be substituted by the associated Goldstone boson allowing an error

$$\varepsilon_L^\mu(k) = \frac{k^\mu}{M_W} + \mathcal{O}\left(\frac{M_W}{\sqrt{s}}\right). \quad (25)$$

This error assumed at the TeV scale, the cut off of our theory, is then lower than 10%.

The calculation carried out in Ref. [15] just allowed the longitudinal part of the gauge bosons running inside the loops but for this study a full $\mathcal{O}(g)$ calculation is performed and the number of diagrams that needs to be taken into account scales to more than 1500. This calculation has been done with the help of FeynArts [60], FeynCalc [61] and FeynHelpers [62] Mathematica packages. These routines are able to evaluate the one loop integrals in the Passarino-Veltman notation[63] and extract just the divergent part of the diagrams when is required.

The expressions (10)-(13) are also valid within the equivalence theorem but now the symmetry will be manifest at the level of the Mandelstam variables themselves in the absence

of polarization vectors that do not transform as four vectors under Lorentz transformations [16], which is a nice simplification.

After use of the ET we have to consider the (real part of) the following processes:

$$1. \quad \omega^+ \omega^- \rightarrow zz$$

From the isospin point of view, this is the fundamental amplitude for elastic $\omega\omega$ scattering. In this process 294 1PI diagrams participate at one loop level. The divergences that appear need to be absorbed by redefinitions of coefficients of the tree level amplitude up to NLO. When the W_L are replaced by the ω , following the equivalence theorem, the amplitude tree-level amplitude reads

$$\begin{aligned} \mathcal{A}_{tree}^{\omega\omega} = & -\frac{s(M_h^2 - s(1 - a^2))}{(s - M_h^2)v^2} + \frac{4}{v^4}(a_4(t^2 + u^2) + 2a_5s^2) + \left[\frac{g^2}{4} \frac{u - s}{t - M_W^2} \left(1 + \frac{8a_3t}{v^2} \right) \right. \\ & \left. + u \iff t \right] \end{aligned} \quad (26)$$

with the infinitesimal substitutions

$$\begin{aligned} M_h^2 &\rightarrow M_h^2 + \delta M_h^2, & M_W^2 &\rightarrow M_W^2 + \delta M_W^2, & v^2 &\rightarrow v^2 + \delta v^2, \\ a &\rightarrow a + \delta a, & a_4 &\rightarrow a_4 + \delta a_4, & a_5 &\rightarrow a_5 + \delta a_5, & a_3 &\rightarrow a_3 + \delta a_3 \end{aligned} \quad (27)$$

Besides, a redefinition of the Goldstone's fields in the Lagrangian needs to be used for the divergent corrections of the external legs

$$\{\omega^\pm, z\} \rightarrow \sqrt{Z_{\omega^\pm, z}} \{\omega^\pm, z\} \approx (1 + \frac{1}{2} \delta Z_{\omega^\pm, z}) \{\omega^\pm, z\} \quad (28)$$

$$2. \quad \omega^+ \omega^- \rightarrow hh$$

This scattering requires computing 505 one loop 1PI diagrams. The tree level amplitude is

$$\begin{aligned} \mathcal{A}_{tree}^{\omega h} = & -b \frac{s}{v^2} - \frac{6a\lambda_3s}{s - M_h^2} - \left[\frac{g^2}{4(t - M_W^2)} \left(2a^2s + \frac{a^2}{t}(t - M_h^2)^2 \right) + t \iff u \right] \\ & - \frac{1}{v^2} \left[\frac{\zeta ag^2}{2(t - M_W^2)} (t(s - u) + M_h^4) + t \iff u \right] - \frac{1}{v^2} \left[\frac{a^2}{t}(t - M_h^2)^2 \right. \\ & \left. + t \iff u \right] + \frac{1}{v^4} (2\delta s(s - M_h^2) + \eta((t - M_h^2)^2 + (u - M_h^2))) \end{aligned} \quad (29)$$

To get rid of the divergences of this process, the following substitutions for the couplings are needed

$$\begin{aligned} M_h^2 &\rightarrow M_h^2 + \delta M_h^2, & M_W^2 &\rightarrow M_W^2 + \delta M_W^2, & v^2 &\rightarrow v^2 + \delta v^2, & a &\rightarrow a + \delta a \\ b &\rightarrow b + \delta b, & \lambda_3 &\rightarrow \lambda_3 + \delta \lambda_3, & \delta &\rightarrow \delta + \delta \delta, & \eta &\rightarrow \eta + \delta \eta, & \zeta &\rightarrow \zeta + \delta \zeta \end{aligned} \quad (30)$$

Now, apart from (28), we will also need the redefinition of the classical Higgs field

$$h \rightarrow \sqrt{Z_h} h \approx (1 + \frac{1}{2} Z_h) h \quad (31)$$

3. $hh \rightarrow hh$

This process at the one loop level contains 654 1PI diagrams and the divergences must be cancelled from the parameters of the amplitude (17) once the usual Mandelstam definitions have been applied.

$$\begin{aligned} \mathcal{A}_{tree}^{hh} = & -6\lambda_4 - 36\lambda_3^2 v^2 \left(\frac{1}{s - M_h^2} + \frac{1}{t - M_h^2} + \frac{1}{u - M_h^2} \right) + \frac{8\gamma}{v^4} \left(\left(\frac{s}{2} - M_h^2 \right)^2 \right. \\ & \left. + \left(\frac{t}{2} - M_h^2 \right)^2 + \left(\frac{u}{2} - M_h^2 \right)^2 \right) \end{aligned} \quad (32)$$

The universal counterterms

$$\begin{aligned} M_h^2 &\rightarrow M_h^2 + \delta M_h^2, & v^2 &\rightarrow v^2 + \delta v^2, & \lambda_3 &\rightarrow \lambda_3 + \delta \lambda_3, \\ \lambda_4 &\rightarrow \lambda_4 + \delta \lambda_4, & \gamma &\rightarrow \gamma + \delta \gamma \end{aligned} \quad (33)$$

are required for absorbing the divergences plus the Higgs redefinition (31).

B. Determination of counterterms

The real absorptive part has both finite and divergent parts. The divergences are reabsorbed in the amplitudes via new parameters from redefinitions of couplings and fields of the bare theory (5) given in the previous subsections.

All these new parameters, the counterterms of our theory, are not uniquely defined and depend on the choice of physical inputs to define the finite part of the amplitude. In this study the so-called on-shell (OS) scheme (see e.g. [64]) has been used. It states that the physical

mass is placed in the pole of the renormalized propagator with residue 1. This means

$$Re \left[\Pi_{h,W_T}(q^2 = M_{h,W_T}^2) - \delta M_{h,W_T}^2 \right] = 0, \quad Re \left[\frac{d\Pi_{h,\omega,W}}{dq^2}(q^2 = M_{h,W,\omega}^2) + \delta Z_{h,W,\omega} \right] = 0 \quad (34)$$

where $\Pi(q^2)$ is the one loop correction to the respective propagator. The OS, first used in the context of LEP physics, has the advantage that many relevant radiative corrections involve only two-point functions. This is obvious for the masses and wave function renormalization. After the splittings $\delta M_{h,W}^2 = \delta \bar{M}_{h,W}^2 + \delta M_{h,W,div}^2$ and $\delta Z_{h,\omega} = \delta \bar{Z}_{h,\omega} + \delta Z_{h,\omega,div}$ we obtain

$$\begin{aligned} \delta M_{h,div}^2 &= \frac{\Delta}{32\pi^2 v^2} (3 [6(2a^2 + b) M_W^4 - 6a^2 M_W^2 M_h^2 + (3d_3^2 + d_4 + a^2) M_h^4]), \\ \delta M_{W,div}^2 &= \frac{\Delta}{48\pi^2 v^2} (M_W^2 [3(b - a^2) M_h^2 + (-69 + 10a^2) M_W^2]), \\ \delta Z_{h,div} &= \frac{\Delta}{16\pi^2 v^2} (3a^2 (3M_W^2 - M_h^2)), \\ \delta Z_{\omega,div} &= \frac{\Delta}{16\pi^2 v^2} ((b - a^2) M_h^2 + 3(a^2 + 2) M_W^2) \end{aligned} \quad (35)$$

where $\Delta \equiv \frac{1}{\epsilon} + \log(4\pi) + \gamma_E$ and the dimensionality is set to $4 + 2\epsilon$.

The one loop level propagator mixing between the gauge boson and its associated Goldstone is protected by the gauge fixing condition in (6) and no extra counterterms will be needed for this. In the absence of electromagnetic interactions assuming an exact custodial symmetry, no $Z - \gamma$ mixing in the gauge propagator can occur either.

Besides, the condition of vanishing tadpole is assumed. There is an extra counterterm δT that cancels the Higgs tadpole contribution at one loop satisfying the usual relation [15]

$$\delta T = -v (\delta M_h^2 - 2v^2 \delta \lambda - 2\lambda \delta v^2) = -\mathcal{A}_{tad}^h \quad (36)$$

With our parametrization for the Higgs potential, λ does not appear in any of the processes but its counterterm can be determined using (36) once δM_h^2 and δv^2 are obtained.

The matrix field (1) containing the goldstones in the HEFT should retain its unitarity and hence it cannot receive any multiplicative renormalization. Perturbatively, the redefinitions of the $n - th$ term of the expansion of U

$$\frac{1}{n!} \left(i \frac{\omega}{v} \right)^n \rightarrow \frac{1}{n!} \left(i \frac{\omega}{v} \right)^n + \frac{1}{2(n-1)!} \left(\delta Z_\omega - \frac{\delta v^2}{v^2} \right) \left(i \frac{\omega}{v} \right)^n \quad (37)$$

It turns out that to absorb the one-loop divergences, the counterterms for the Goldstone fields ($\sqrt{Z_\omega}$) and the vev ($\sqrt{\delta v^2}$) are equal so they cancel each other at every order in the

expansion. The *finite* part of $\sqrt{\delta v^2}$ is fixed, at every order, by the condition

$$\delta Z_\omega = \frac{\delta v^2}{v^2}. \quad (38)$$

The complete list of counterterms allowing us to get rid of the divergences of the three amplitudes in the previous subsections is

$$\begin{aligned} \delta a &= \frac{\Delta}{32\pi^2 v^2} (6a(-2a^2 + b + 1)M_W^2 + (5a^3 - a(2 + 3b) - 3d_3(a^2 - b))M_h^2), \\ \delta v_{div}^2 &= \frac{\Delta}{16\pi^2} ((b - a^2)M_h^2 + 3(a^2 + 2)M_W^2), \\ \delta b &= \frac{\Delta}{32\pi^2 v^2} (6(3a^4 - 6a^2b + b(b + 2))M_W^2 \\ &\quad - (a(12 - 19a) + b + a(a(3a(7a - 6) - 5) + 6) + 2b^2 + b)M_h^2), \\ \delta \lambda_{div} &= \frac{\Delta}{64\pi^2 v^4} ((5a^2 - 2b + 3(d_3(3d_3 - 1) + d_4))M_h^4 - 12(2a^2 + 1)M_W^2 M_h^2 \\ &\quad + 18(a(2a - 1) + b)M_W^4), \\ \delta \lambda_3 &= \frac{\Delta}{64\pi^2 v^4} (36abM_W^4 + 6(3a^3 - 3ab - d_3(5a^2 + 1))M_W^2 M_h^2 \\ &\quad + (-9a^3 + 3ab + d_3(10a^2 - b) + 9d_3 d_4)M_h^4), \\ \delta \lambda_4 &= \frac{\Delta}{64\pi^2 v^4} (36b^2 M_W^4 - 12(a^2 - b)(8a^2 - 2b - 9ad_3)M_W^2 M_h^2 \\ &\quad + (96a^4 + 4b^2 - d_3(114a^3 - 42ab) + 9d_4^2 + a^2(-64b + 27d_3^2 + 12d_4))M_h^4), \\ \delta a_3 &= -\frac{\Delta}{384\pi^2} (1 - a^2), \quad \delta a_4 = -\frac{\Delta}{192\pi^2} (1 - a^2)^2, \\ \delta a_5 &= -\frac{\Delta}{768\pi^2} (5a^4 - 2a^2(3b + 2) + 3b^2 + 2), \\ \delta \gamma &= -\frac{\Delta}{64\pi^2} 3(b - a^2)^2, \quad \delta \delta = -\frac{\Delta}{192\pi^2} (b - a^2)(7a^2 - b - 6), \quad \delta \eta = -\frac{\Delta}{48\pi^2} (b - a^2)^2, \\ \delta \zeta &= \frac{\Delta}{96\pi^2} a(b - a^2). \end{aligned} \quad (39)$$

C. Cross-checks and comparison with previous results

All these counterterms above have the correct SM limit. When $a = b = d_3 = d_4 = 1$, all the parameters that are not present in the SM vanish, and we are left with δv_{div}^2 , $\delta \lambda_{div}$, $\delta \lambda_3$ and $\delta \lambda_4$. In the SM limit, $\delta \lambda$, $\delta \lambda_3$ and $\delta \lambda_4$ have been checked to be exactly equal, as it should since they all derive from the unique SM Higgs potential coupling λ present in the tadpole, triple and quartic self-couplings. In particular

$$\delta \lambda_{div,SM} = \delta \lambda_{3,SM} = \delta \lambda_{4,SM} = \frac{3\Delta}{16\pi^2 v^4} (3M_W^4 - 3M_W^2 M_h^2 + M_h^4). \quad (40)$$

As explained before, it can be seen just by direct comparison with (35), that the relation (38) is satisfied.

We can also compare our counterterms with partial results previously reported in the literature. As mentioned before, the authors in Ref [15] made a complete study of the elastic $\omega\omega$ scattering at one loop level, allowing only longitudinal modes in the internal lines. This is, they set $g = 0$ for the whole process and therefore they set for the vector boson mass the value $M_W = 0$. Our results (35) and (39) have been checked with those relevant for the process in [15] in the limit $M_W = 0$.

A cruder approximation was taken in [65] where they studied all the processes including the $I = 0$ final states but, besides setting $g = 0$ and neglecting physical vector bosons in the loops, the authors took the limit $M_h = 0$. In this limit where the self interactions of the Higgs are absent, there is no need for redefinitions of a, b and v to absorb the one loop divergences and we are left with $a_4, a_5, \gamma, \delta, \eta$. Our results agree with theirs in the limit $M_W = M_h = 0$.

We have also compared our results with the more recent study [41] where the authors performed a full renormalization of the one loop Green functions involved in elastic $W_L W_L$ scattering. We find our results compatible, with two differences originating from the inclusion by these authors of two $\mathcal{O}(p^4)$ operators,

$$a_{\square\square} \frac{\square h \square h}{v^2}, \quad a_{\square VV} \frac{\square h}{v} \text{Tr}(V_\mu V^\mu), \quad (41)$$

where \square is the d'Alembertian operator. These operators can be reduced by using the equation of motion of the Higgs field at leading order (omitting the leptonic contribution)

$$\square h = -\frac{v^2}{4} \text{Tr}(V_\mu V^\mu) \frac{2a}{v} + M_h^2 h + \dots \quad (42)$$

and are for our purposes redundant. The first of these two operator enters directly in the renormalization of the propagator of the Higgs so, even with the same OS renormalization condition as ours, δZ_h and δM_h^2 differ in a consistent way. After using the e.o.m., both operators are actually redundant and change the coefficients a and a_5 . Naming their chiral parameters \tilde{a} and \tilde{a}_5 , the following redefinitions make the two set of results compatible.

$$\begin{aligned} a &= \tilde{a} + \frac{2M_h^2}{v^2} (a_{\square VV} - \tilde{a} a_{\square\square}) \\ a_5 &= \tilde{a}_5 - \frac{\tilde{a}}{2} a_{\square VV} + \frac{\tilde{a}^2}{4} a_{\square\square} \end{aligned} \quad (43)$$

One can check easily that all our additional or ‘anomalous’ counterterms do vanish in the SM limit, while this is not so for \tilde{a} and \tilde{a}_5 .

The authors in [6] also obtained the divergences of the HEFT local operators with the heat kernel formalism for the path integral. To this purpose, they needed to make redefinitions of the quantum fields, in particular the Higgs field, so they were present in the canonical normalization. These redefinitions alter the UV divergences of some operators with respect to those in our Lagrangian. All the $\mathcal{O}(p^4)$ divergences, not affected by field renormalizations, have been checked to coincide after some reparametrization of the chiral couplings.

D. Imaginary part: The Optical theorem

The imaginary part of the NLO amplitude is obtained exactly using the Optical Theorem. The fact that some states can go on-shell in the process, forces the presence of a physical cut in the analytic structure of an amplitude that depends on the variable s promoted to a complex quantity. This amplitude is obtained after the analytical continuation to the whole complex plane of the Feynman amplitude depending on the centre of mass energy, a real variable.

Given a physical amplitude $\mathcal{A}(s)$, once we know the discontinuity of the complex amplitude across the physical cut with the usual Cutkosky rules, we find

$$Im \mathcal{A}(s) = \sigma(s) |\mathcal{A}(s)|^2 \quad (44)$$

where $\sigma(s) = \sqrt{1 - \frac{(M_1+M_2)^2}{s}}$ is the two body phase space. This allows us to compute the imaginary part of any amplitude at the one loop level from the tree-level result.

As an example, if we are interested in computing the full $I = 1$ isospin amplitude in the process $W_L^+ W_L^- \rightarrow Z_L Z_L$

$$\mathcal{A}(W_L^+ W_L^- \rightarrow Z_L Z_L) = \mathcal{A}_{tree}^{(2)} + \mathcal{A}_{tree}^{(4)} + \mathcal{A}_{loop}^{(4)} \quad (45)$$

where $\mathcal{A}_{tree}^{(2)} + \mathcal{A}_{tree}^{(4)}$ is the amplitude (15) and $\mathcal{A}_{loop}^{(4)}$ is the full one loop amplitude

$$\mathcal{A}_{loop}^{(4)} = Re \left[\mathcal{A}_{loop}^{(4)}(\omega^+ \omega^- \rightarrow zz) \right] + i\sigma(s) |\mathcal{A}_{tree}^{(2)}|^2 \quad (46)$$

V. UNITARIZATION

Departures from the SM such as those described by the HEFT unavoidably result in a loss of unitarity. Amplitudes typically exhibit a bad ultraviolet behavior leading to cross sections that grow too fast with the energy \sqrt{s} and quickly violate the unitarity bounds. While this is well known, it is sometimes forgotten that this fast growth of the amplitudes results in a hypersensitivity to deviations of the coefficients of the HEFT with respect to their SM values. We analyze this in some more detail in the next subsections.

Once we have built the fixed isospin amplitudes using equation (12), we can obtain the amplitude with J total angular momentum with the corresponding partial wave

$$t_{IJ}(s) = \frac{1}{32K\pi} \int_{-1}^1 d(\cos\theta) P_J(\cos\theta) T_I(s, \cos\theta) \quad (47)$$

using the center of mass relations $t = -(s - 4M_W^2)(1 - \cos\theta)/2$ and $u = -(s - 4M_W^2)(1 + \cos\theta)/2$. K is a constant whose value is $K = 2$ or 1 depending on whether the particles participating in the process are identical or not.

The way we compute the fixed isospin amplitudes using Feynman diagrams from the Lagrangian (5), leads to a perturbative expansion of the form

$$t_{IJ}(s) \approx t_{IJ}^{(2)} + t_{IJ}^{(4)} + \dots \quad (48)$$

which satisfies perturbatively the optical theorem in (44)

$$\begin{aligned} \text{Im} \left(t_{11}^{(2)} \right) &= 0 \\ \text{Im} \left(t_{11}^{(4)} \right) &= \sqrt{1 - \frac{4M_W^2}{s}} |t_{11}^{(2)}|^2 \end{aligned} \quad (49)$$

A. Amplitudes at high energies

In Figure 1 we plot the modulus of the real part of the amplitude computed at the tree plus one-loop level for the process $W_L W_L \rightarrow Z_L Z_L$ for various values of the parameter a . Departures from the SM value $a = 1$ result in a clear bad high-energy behavior. This same behavior is seen in the remaining $2 \rightarrow 2$ processes. For instance the modulus of the real part of the amplitude for the process $W_L W_L \rightarrow hh$ is depicted in Figure 2 for the same values of the parameter a parameterizing the Higgs-vector boson coupling in the HEFT.

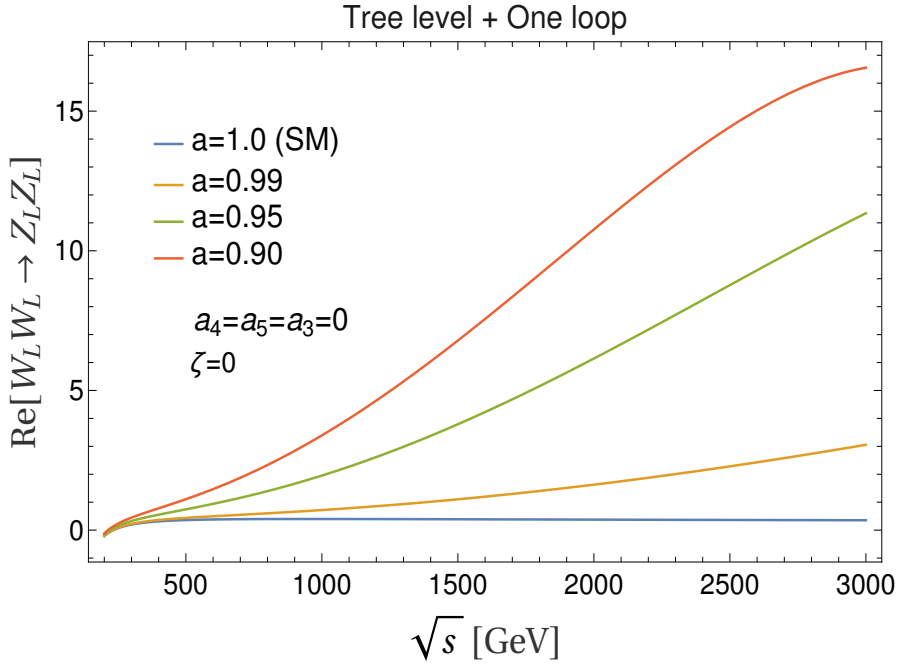


FIG. 1: Plot of the modulus of the real part of the elastic vector boson scattering (VBS) in longitudinal polarization ($W_L W_L \rightarrow Z_L Z_L$) versus the center of mass energy for some values of the chiral parameter a . It can be seen how small departures for the SM value ($a = 1$) leads to a quick violation of unitarity within the HEFT regime of validity. All the $\mathcal{O}(p^4)$ couplings contributing to the process (a_3, a_4, a_5, ζ) are set to zero

On the contrary, this same real part of the $W_L W_L \rightarrow hh$ amplitude (Figure 2) shows a milder dependence on the parameter λ_3 of the Higgs potential. For the SM value $a = 1$, modifying λ_3 does not show obvious signs of bad high-energy behavior. At this level, this derives from the fact that this coupling is momentum independent. Note that this coupling is very poorly constrained so the overall uncertainty of the amplitude is accordingly large.

Higher loop calculations will only worsen the high-energy behavior. It is thus clear that, except for tiny deviations from the SM, as soon as one enters the multi TeV region, the perturbative treatment is unreliable. Therefore, checking for constraints on the anomalous couplings present in the HEFT by just looking at growing cross sections is risky but may be justified (if the deviations are small) or plain wrong (if the anomalous coupling constants deviate significantly from their SM values). It is clear that physical amplitudes —even beyond the SM— are necessarily unitary, meaning that in the HEFT higher loops contributions have

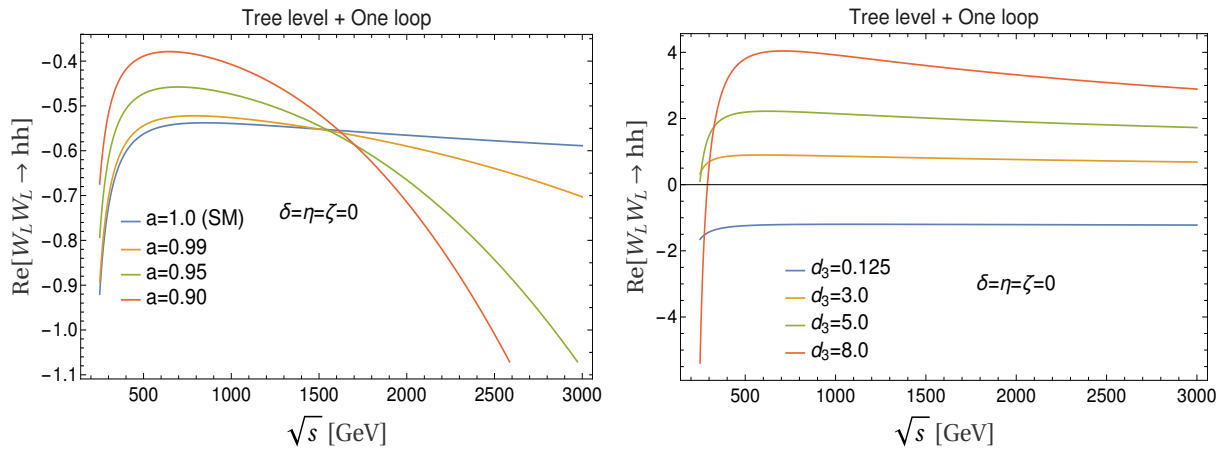


FIG. 2: Plot of the modulus of the real part of the process $W_L W_L \rightarrow hh$ versus the center of mass energy for some values of the chiral parameter a (left) and the trilinear Higgs coupling $\lambda_3 = d_3 \lambda$ (right). It can be seen how departures from the SM case do not lead to bad UV behavior of the amplitude in the second case. In each figure, the remaining parameters do not vary and are set to the corresponding SM values.

to be somehow summed up to render a reasonable high-energy behavior, which of course will be different from the SM one, but still in accordance with the general principles of field theory. We conclude that unitarization is necessary to compare the predictions of the HEFT with those of the SM vis a vis the experiments at very high energies, particularly when we are close to the HEFT UV cutoff.

B. The Inverse Amplitude Method (IAM)

The expansion in terms of the external momentum typically leads very quickly to a violation of unitarity and, in order to make realistic predictions, unitarization techniques need to be used. In our case we choose to make use of the Inverse Amplitude Method (IAM) [18, 20, 22–28] in order to unitarized the partial waves (and, eventually, the amplitudes). The IAM is really successful in predicting the features of the rho meson resonance studying low energy QCD with pion-pion scattering and it has also been extensively used in HEFT analysis.

The method consists in building the following IAM amplitude up to NLO

$$t_{IJ}^{IAM} \simeq \frac{\left(t_{IJ}^{(2)}\right)^2}{t_{IJ}^{(2)} - t_{IJ}^{(4)}} \quad (50)$$

which perturbatively satisfies (48) and the desired unitarity condition $t_{IJ}(s) = \frac{i}{2}(1 - \eta(s)e^{2i\delta(s)})$, where $0 < \eta < 1$ is the inelasticity.

A pole in the unitary amplitude (50) appears when, for some complex value of s_R (51),

$$t_{IJ}^{(2)}(s_R) - t_{IJ}^{(4)}(s_R) = 0 \quad (51)$$

This pole, if present, is interpreted as a resonance with quantum numbers I, J and features M_R and Γ_R , these last given *a la Wigner* by the position of the pole in the complex plane $s_R = (M_R - \frac{i}{2}\Gamma_R)^2$. We will consider for this study and future ones only the lowest partial wave in $I = 0, 1$ channels and refer to these resonances as scalar-isoscalar for the poles in t_{00}^{IAM} and vector-isovector for t_{11}^{IAM} .

One nicety of the IAM, besides assuring unitarity, is that the poles can be interpreted as dynamically generated resonances appearing after the re-summation of infinite bubbles chain $WW \rightarrow ZZ \rightarrow WW \rightarrow \dots \rightarrow ZZ$ (in the $I = 1$ channel) as it can be understood diagrammatically from the perturbative expansion of (50).

In the $I = 0$ channel two Higgs intermediate states are possible and for that one needs the machinery of coupled channels.

The IAM method can be extended to the coupled channel case too (see [25, 66]), particularly if all the different channels have the same thresholds. From the perturbative expansion

$$T_{IJ} = T_{IJ}^{(2)} + T_{IJ}^{(4)} + \dots \quad (52)$$

a natural generalization of the IAM method gives

$$T_{IJ}^{IAM} = T_{IJ}^{(2)}(T_{IJ}^{(2)} - T_{IJ}^{(4)})^{-1}T_{IJ}^{(2)} \quad (53)$$

which satisfies exact multichannel elastic unitarity on the right cut

$$Im T_{IJ}^{IAM} = T_{IJ}^{IAM}(T_{IJ}^{IAM})^\dagger. \quad (54)$$

The IAM has been extensively used to describe low-energy meson-meson scattering where it has proven to be extremely successful. With a very small set of parameters, it is able

to describe many different channels including their first resonances [17, 20, 25, 66]. In the case of coupled channels, the different amplitude matrix elements (partial waves) $(T_{IJ})_{ij}(s)$ correspond to different reactions having the same quantum numbers IJ . Clearly, if there is a resonance in one of the channels it should appear also in all the others since physically these resonances can be produced in any of the reactions.

While for single channel unitarization the IAM is well grounded and relies on a minimal set of assumptions (see e.g. [17, 21, 25, 66]), there is no really unambiguous way of applying the IAM to the case where there are coupled channels with different thresholds. We shall adhere to the simplest choice that consists in assuming the previous expressions to remain valid also in the present analysis. This can be justified heuristically on the grounds that M_W is not too different from M_h . This is again a good justification of the need to include all polarizations of the vector boson with a mass M_W in the calculation.

In addition, it should be stated that the decoupling of the two $I = 0$ channels in the case $a^2 = b$ taking place when the equivalence theorem is used and physical W_L are replaced by the corresponding Goldstone bosons does not hold in the exact calculation.

The results for the $IJ = 00$ channel will be reported in a separate publication. Here we will concentrate in the modifications that the inclusion of the transverse mode propagation of the vector bosons with a mass M_W and the appearance of new effective couplings in the HEFT induce in the $IJ = 11$ channel.

C. Vector resonances

In order to see the relevance of including the propagation of transverse modes, we focus on vector resonances with quantum numbers $I, J = 1, 1$ in VBS. We shall compare the new results with those obtained previously.

From equations (11) and (12), the fixed isospin amplitudes in the chiral expansion, $T_1^{(2)}$ and $T_1^{(4)}$ are obtained. $T_1^{(2)}$ using $\mathcal{A}_{tree}^{(2)}(p_1, p_2, p_3, p_4)$ and $T_1^{(4)}$ with $\mathcal{A}_{tree}^{(4)}(p_1, p_2, p_3, p_4) + Re[\mathcal{A}_{loop}(\omega^+ \omega^- \rightarrow zz)](p_1, p_2, p_3, p_4)$. Using equation (47) and (49) perturbatively, we find

the partial wave for $I, J = 1, 1$

$$\begin{aligned} t_{11}^{(2)} &= \frac{1}{64\pi} \int_{-1}^1 d(\cos \theta) \cos \theta T_1^{(2)}(s, \cos \theta) \\ \text{Re} \left[t_{11}^{(4)} \right] &= \frac{1}{64\pi} \int_{-1}^1 d(\cos \theta) \cos \theta T_1^{(4)}(s, \cos \theta) \\ \text{Im} \left[t_{11}^{(4)} \right] &= \sqrt{1 - \frac{4M_W^2}{s}} |t_{11}^{(2)}|^2 \end{aligned} \quad (55)$$

where the Legendre polynomial $P_1(\cos \theta) = \cos \theta$ has been used.

The vector-isovector resonances, if present, are located by searching for poles of the unitary IAM amplitude (50) i.e. looking for solutions of equation (51).

Let us first of all investigate how the proper inclusion of the transverse modes (i.e. $g \neq 0$) influence the results obtained in the extreme ET limit. Below we provide results for $g = 0$ and $g = 2M_W/v$. The benchmark points correspond to those used in [19]. As it can be seen

$\sqrt{s_V} (\text{GeV})$	$g = 0$	$g \neq 0$	a	$a_4 \cdot 10^4$	$a_5 \cdot 10^4$
BP1	$1476 - \frac{i}{2}14$	$1503 - \frac{i}{2}13$	1	3.5	-3
BP2	$2039 - \frac{i}{2}21$	$2087 - \frac{i}{2}20$	1	1	-1
BP3	$2473 - \frac{i}{2}27$	$2540 - \frac{i}{2}27$	1	0.5	-0.5
BP1'	$1479 - \frac{i}{2}42$	$1505 - \frac{i}{2}44$	0.9	9.5	-6.5
BP2'	$1981 - \frac{i}{2}97$	$2025 - \frac{i}{2}98$	0.9	5.5	-2.5
BP3'	$2481 - \frac{i}{2}183$	$2547 - \frac{i}{2}183$	0.9	4	-1

TABLE II: Values for the location of the vector poles $\sqrt{s_V} = M_V - \frac{i}{2}\Gamma_V$ found in all the benchmark points of reference [19] once the transverse modes are included ($g \neq 0$).

ceteris paribus the inclusion of the gauge boson masses systematically increases the masses of the resonances by a few per cent. The modifications in the widths are not significant. In these calculations $b = a^2$, and both a_3 and ζ have been set to zero.

D. Checking unitarity

As a check of the good unitarity behavior of the amplitudes obtained in the IAM method and the validity of the approximations made we plot the partial wave for complex values of the kinematical variable s in the $IJ = 11$ channel. There are no threshold in this channel

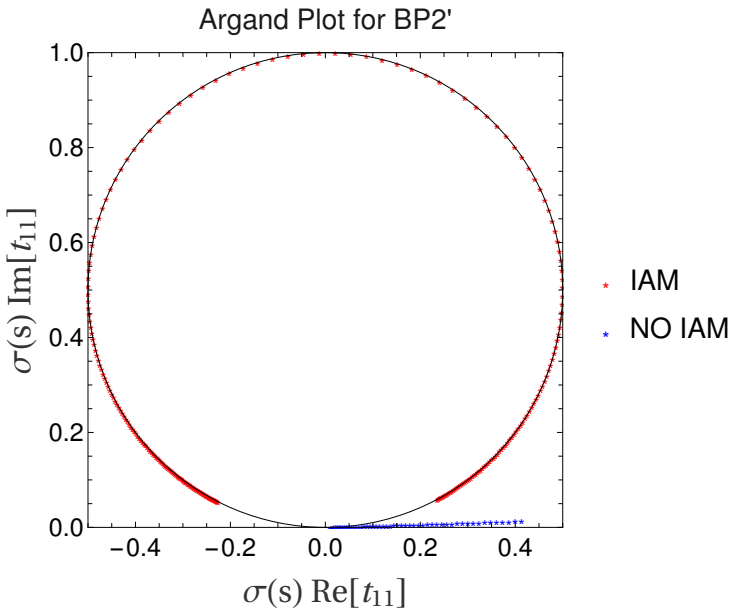


FIG. 3: Argand plot showing the unitary VBS amplitude (red points) for the values of BP2' from Table II. Due to the elasticity of the process, the IAM amplitude lies exactly on the unitarity limit, i.e, the circumference of radius 1/2 centered at $(0, 1/2)$. The amplitude before applying the IAM is also present (blue points) and obviously lies entirely outside the unitarity condition.

beyond the elastic channel and the results must lie accordingly in a circumference of radius 1/2 centered at $s = i/2$. This is shown in Fig. 3. We also plot the results obtained for the same $IJ = 11$ channel in perturbation theory —without resummation. They obviously violate the unitarity bound. The plot correspond to the values of the Benchmark point BP2' from Table II, corresponding to $a = 0.9$, $a_4 = 5.5 \cdot 10^{-4}$ and $a_5 = -2.5 \cdot 10^{-4}$, within the recent CMS experimental bounds of Table I.

E. Influence of the new HEFT constants

The inclusion of transverse modes in the calculation of the dispersive real part of the amplitude leads unavoidably to consider the case where $M \neq 0$. We have seen how this changes to some extent the location and widths of the amplitudes. On the other hand, the inclusion of the transverse modes leads to the appearance of new counterterms in the HEFT. In the channel $IJ = 11$ two new low energy ('anomalous') couplings appear: a_3 and ζ . Let us see how their presence may affect the previous results.

For this analysis we focus in the four lightest resonances of Table II. This is $BP1$, $BP2$, $BP1'$ and $BP2'$. We see from the previous results that, of the two new parameters (not previously

$\sqrt{s_V}$ (GeV)	$a_3 = 0$	$a_3 = 0.1$	$a_3 = -0.1$	$a_3 = 0.01$	$a_3 = -0.01$
BP1	$1503 - \frac{i}{2}13$	$1795 - \frac{i}{2}11$	$1215 - \frac{i}{2}15$	$1532 - \frac{i}{2}13$	$1474 - \frac{i}{2}13$
BP2	$2087 - \frac{i}{2}20$	$2721 - \frac{i}{2}15$	$1505 - \frac{i}{2}23$	$2150 - \frac{i}{2}19$	$2025 - \frac{i}{2}21$
BP1'	$1505 - \frac{i}{2}44$	$1663 - \frac{i}{2}46$	$1335 - \frac{i}{2}43$	$1520 - \frac{i}{2}44$	$1488 - \frac{i}{2}44$
BP2'	$2025 - \frac{i}{2}98$	$2278 - \frac{i}{2}104$	$1752 - \frac{i}{2}89$	$2052 - \frac{i}{2}98$	$1999 - \frac{i}{2}97$

TABLE III: Values for the location of the vector poles $\sqrt{s_V} = M_V - \frac{i}{2}\Gamma_V$ found in all the benchmark points of reference [19] for different values of a_3 and $g \neq 0$. The chiral parameter ζ is set to zero.

$\sqrt{s_V}$ (GeV)	$\zeta = 0$	$\zeta = 0.1$	$\zeta = -0.1$	$\zeta = 0.01$	$\zeta = -0.01$
BP1	$1503 - \frac{i}{2}13$	$1637 - \frac{i}{2}13$	$1377 - \frac{i}{2}14$	$1516 - \frac{i}{2}13$	$1489 - \frac{i}{2}13$
BP2	$2087 - \frac{i}{2}20$	$2393 - \frac{i}{2}18$	$1809 - \frac{i}{2}22$	$2117 - \frac{i}{2}20$	$2058 - \frac{i}{2}21$
BP1'	$1505 - \frac{i}{2}44$	$1570 - \frac{i}{2}46$	$1439 - \frac{i}{2}43$	$1510 - \frac{i}{2}45$	$1497 - \frac{i}{2}45$
BP2'	$2025 - \frac{i}{2}98$	$2136 - \frac{i}{2}100$	$1915 - \frac{i}{2}94$	$2036 - \frac{i}{2}98$	$2014 - \frac{i}{2}97$

TABLE IV: Values for location of the vector poles $\sqrt{s_V} = M_V - \frac{i}{2}\Gamma_V$ found in all the benchmark points of reference [19] for different values of ζ and $g \neq 0$. The chiral parameter a_3 is set to zero.

considered in unitarization analysis), a_3 is most relevant as it can be seen in tables III and IV. Positive values of a_3 tend to increase the mass of the vector resonance and make it even narrower, making its detection harder. Negative values of a_3 work in the opposite direction. Although the bounds on a_3 allow it, the value $|a_3| = 0.1$ may be too large, and we also provide M_V and Γ_V for $|a_3| = 0.01$. If a_3 happened to be of the same order as the current bounds for a_4 and a_5 , its effect would be subleading. The influence of ζ appears to be less than that of a_3 but the qualitative behavior remains.

VI. CONCLUSIONS

One of the main results of this paper is the determination of the one-loop quantum corrections to all the relevant $2 \rightarrow 2$ processes that are relevant to two-Higgs production via the scattering of electroweak gauge bosons in the HEFT. The calculation has been

explicitly performed in the 't Hooft-Landau gauge, although physical amplitudes are gauge independent.

In the literature, results only exist for some specific cases. In our work, for the first time, a full and complete diagrammatic computation of all the $2 \rightarrow 2$ processes relevant for two-Higgs production is presented. In the one-loop calculation, both transverse and longitudinal polarized modes are included. In the on-shell scheme this necessarily leads to considering the physical values for the Higgs and weak gauge boson masses³. The resulting amplitudes are then unitarized and we analyze the characteristics of the dynamical resonances appearing. An interesting result is that, after unitarization of the partial waves, the effect of including the gauge boson masses is small but significant increasing the mass of the vector resonances typically in the range 2 to 3 %. The widths are unchanged.

The introduction of the transverse degrees of freedom of the gauge bosons also implies the need to consider additional effective couplings that had not been previously considered in unitarization studies. In elastic $WW \rightarrow WW$ scattering, there are two new effective couplings that become relevant. While traditionally the effective couplings a_4 and a_5 have been regarded as driving the masses of dynamical resonances, it turns out that the coupling a_3 (that plays a role only if the *a priori* subdominant transverse modes are included) is relevant too. It should also be mentioned that while a_4 and a_5 are by now fairly constrained by LHC analysis, the bounds on a_3 are still rather loose. This makes the present study particularly relevant, we believe.

In the present paper, we have focused on the impact of the new contributions in the vector-isovector channel and have postponed the consideration of the more involved scalar-isoscalar one to a future publication. Unitarization of the latter, that requires a full use of the coupled channel formalism, is most relevant in order to be able to constraint some of the Higgs couplings.

³ However, in order to be able to use safely exact isospin relations we work in the custodial limit neglecting electromagnetism, i.e. $g' = 0$.

Acknowledgements

We thank Oscar Catà and Rafael Delgado for useful discussions. We acknowledge financial support from the State Agency for Research of the Spanish Ministry of Science and Innovation through the “Unit of Excellence María de Maeztu 2020-2023” award to the Institute of Cosmos Sciences (CEX2019-000918-M) and from PID2019-105614GB-C21 and 2017-SGR-929 grants.

- [1] G. Aad et al. (ATLAS), *Phys. Lett. B* **716**, 1 (2012), 1207.7214.
- [2] S. Chatrchyan et al. (CMS), *Phys. Lett. B* **716**, 30 (2012), 1207.7235.
- [3] G. F. Giudice, C. Grojean, A. Pomarol, and R. Rattazzi, *JHEP* **06**, 045 (2007), hep-ph/0703164.
- [4] R. Alonso, M. B. Gavela, L. Merlo, S. Rigolin, and J. Yepes, *Phys. Lett. B* **722**, 330 (2013), [Erratum: *Phys.Lett.B* 726, 926 (2013)], 1212.3305.
- [5] A. Pich, I. Rosell, and J. J. Sanz-Cillero, *Phys. Rev. Lett.* **110**, 181801 (2013), 1212.6769.
- [6] G. Buchalla, O. Catà, and C. Krause, *Nucl. Phys. B* **880**, 552 (2014), [Erratum: *Nucl.Phys.B* 913, 475–478 (2016)], 1307.5017.
- [7] R. Contino, M. Ghezzi, C. Grojean, M. Muhlleitner, and M. Spira, *JHEP* **07**, 035 (2013), 1303.3876.
- [8] G. Buchalla, O. Cata, A. Celis, and C. Krause, *Nucl. Phys. B* **917**, 209 (2017), 1608.03564.
- [9] A. Pich (2018), 1804.05664.
- [10] D. Espriu and B. Yencho, *Phys. Rev. D* **87**, 055017 (2013), 1212.4158.
- [11] P. Arnan, D. Espriu, and F. Mescia, *Phys. Rev. D* **93**, 015020 (2016), 1508.00174.
- [12] A. Pich, I. Rosell, J. Santos, and J. J. Sanz-Cillero, *Phys. Rev. D* **93**, 055041 (2016), 1510.03114.
- [13] A. Pich, I. Rosell, J. Santos, and J. J. Sanz-Cillero, *JHEP* **04**, 012 (2017), 1609.06659.
- [14] A. Pich, I. Rosell, and J. J. Sanz-Cillero, *Phys. Rev. D* **102**, 035012 (2020), 2004.02827.
- [15] D. Espriu, F. Mescia, and B. Yencho, *Phys. Rev. D* **88**, 055002 (2013), 1307.2400.
- [16] D. Espriu and F. Mescia, *Phys. Rev. D* **90**, 015035 (2014), 1403.7386.
- [17] R. L. Delgado, A. Dobado, and F. J. Llanes-Estrada, *Phys. Rev. D* **91**, 075017 (2015),

1502.04841.

[18] T. Corbett, O. J. P. Éboli, and M. C. Gonzalez-Garcia, Phys. Rev. D **93**, 015005 (2016), 1509.01585.

[19] R. L. Delgado, A. Dobado, D. Espriu, C. Garcia-Garcia, M. J. Herrero, X. Marcano, and J. J. Sanz-Cillero, JHEP **11**, 098 (2017), 1707.04580.

[20] C. Garcia-Garcia, M. Herrero, and R. A. Morales, Phys. Rev. D **100**, 096003 (2019), 1907.06668.

[21] A. Salas-Bernárdez, F. J. Llanes-Estrada, J. Escudero-Pedrosa, and J. A. Oller, SciPost Phys. **11**, 020 (2021), 2010.13709.

[22] A. Dobado and J. R. Pelaez, Phys. Rev. D **65**, 077502 (2002), hep-ph/0111140.

[23] F. Guerrero and J. A. Oller, Nucl. Phys. B **537**, 459 (1999), [Erratum: Nucl.Phys.B 602, 641–643 (2001)], hep-ph/9805334.

[24] J. A. Oller, E. Oset, and J. R. Pelaez, Phys. Rev. D **59**, 074001 (1999), [Erratum: Phys.Rev.D 60, 099906 (1999), Erratum: Phys.Rev.D 75, 099903 (2007)], hep-ph/9804209.

[25] J. A. Oller, E. Oset, and J. R. Pelaez, Phys. Rev. Lett. **80**, 3452 (1998), hep-ph/9803242.

[26] A. Dobado and J. R. Pelaez, Phys. Rev. D **56**, 3057 (1997), hep-ph/9604416.

[27] A. Dobado, M. J. Herrero, and T. N. Truong, Phys. Lett. B **235**, 134 (1990).

[28] T. N. Truong, Phys. Rev. Lett. **61**, 2526 (1988).

[29] *2020 Update of the European Strategy for Particle Physics* (CERN Council, Geneva, 2020), ISBN 978-92-9083-575-2.

[30] A. Dobado and D. Espriu, Prog. Part. Nucl. Phys. **115**, 103813 (2020), 1911.06844.

[31] H.-J. He, Y.-P. Kuang, and X.-y. Li, Phys. Lett. B **329**, 278 (1994), hep-ph/9403283.

[32] C. Grosse-Knetter and I. Kuss, Z. Phys. C **66**, 95 (1995), hep-ph/9403291.

[33] A. Dobado and J. R. Pelaez, Phys. Lett. B **329**, 469 (1994), [Addendum: Phys.Lett.B 335, 554 (1994)], hep-ph/9404239.

[34] A. Dobado and J. R. Peláez, Nucl. Phys. B **425**, 110 (1994), [Erratum: Nucl.Phys.B 434, 475–475 (1995)], hep-ph/9401202.

[35] M. S. Chanowitz and M. K. Gaillard, Nucl. Phys. B **261**, 379 (1985).

[36] G. J. Gounaris, R. Kogerler, and H. Neufeld, Phys. Rev. D **34**, 3257 (1986).

[37] B. W. Lee, C. Quigg, and H. B. Thacker, Phys. Rev. D **16**, 1519 (1977).

[38] J. M. Cornwall, D. N. Levin, and G. Tiktopoulos, Phys. Rev. D **10**, 1145 (1974), [Erratum:

Phys. Rev. D 11, 972 (1975)].

[39] G. Buchalla, O. Catà, A. Celis, M. Knecht, and C. Krause (2020), 2004.11348.

[40] G. Buchalla, O. Cata, A. Celis, M. Knecht, and C. Krause, Nucl. Phys. B **928**, 93 (2018), 1710.06412.

[41] M. J. Herrero and R. A. Morales (2021), 2107.07890.

[42] A. Dobado, D. Espriu, and M. J. Herrero, Phys. Lett. B **255**, 405 (1991).

[43] G. Altarelli, R. Barbieri, and F. Caravaglios, Nucl. Phys. B **405**, 3 (1993).

[44] M. E. Peskin and T. Takeuchi, Phys. Rev. D **46**, 381 (1992).

[45] R. Alonso, E. E. Jenkins, and A. V. Manohar, JHEP **08**, 101 (2016), 1605.03602.

[46] J. de Blas, O. Eberhardt, and C. Krause, JHEP **07**, 048 (2018), 1803.00939.

[47] G. Aad et al. (ATLAS), JHEP **07**, 108 (2020), [Erratum: JHEP 01, 145 (2021), Erratum: JHEP 05, 207 (2021)], 2001.05178.

[48] A. M. Sirunyan et al. (CMS), JHEP **03**, 257 (2021), 2011.12373.

[49] M. Tanabashi et al. (Particle Data Group), Phys. Rev. D **98**, 030001 (2018).

[50] E. da Silva Almeida, A. Alves, N. Rosa Agostinho, O. J. P. Éboli, and M. C. Gonzalez-Garcia, Phys. Rev. D **99**, 033001 (2019), 1812.01009.

[51] A. M. Sirunyan et al. (CMS), Phys. Lett. B **795**, 281 (2019), 1901.04060.

[52] A. M. Sirunyan et al. (CMS), Phys. Lett. B **798**, 134985 (2019), 1905.07445.

[53] M. Aaboud et al. (ATLAS), Phys. Rev. D **95**, 032001 (2017), 1609.05122.

[54] O. J. P. Eboli, M. C. Gonzalez-Garcia, and J. K. Mizukoshi, Phys. Rev. D **74**, 073005 (2006), hep-ph/0606118.

[55] O. J. P. Éboli and M. C. Gonzalez-Garcia, Phys. Rev. D **93**, 093013 (2016), 1604.03555.

[56] M. Rauch (2016), 1610.08420.

[57] Tech. Rep., ATLAS Collaboration, CERN (2019), URL <http://cds.cern.ch/record/2693958>.

[58] M. J. Herrero and E. Ruiz Morales, Nucl. Phys. B **418**, 431 (1994), hep-ph/9308276.

[59] M. Herrero and R. A. Morales, Phys. Rev. D **102**, 075040 (2020), 2005.03537.

[60] T. Hahn, Comput. Phys. Commun. **140**, 418 (2001), hep-ph/0012260.

[61] V. Shtabovenko, R. Mertig, and F. Orellana, Comput. Phys. Commun. **256**, 107478 (2020), 2001.04407.

[62] V. Shtabovenko, Comput. Phys. Commun. **218**, 48 (2017), 1611.06793.

- [63] G. Passarino and M. J. G. Veltman, Nucl. Phys. B **160**, 151 (1979).
- [64] A. Grozin, in *3rd Dubna International Advanced School of Theoretical Physics* (2005), hep-ph/0508242.
- [65] R. L. Delgado, A. Dobado, and F. J. Llanes-Estrada, JHEP **02**, 121 (2014), 1311.5993.
- [66] A. Gomez Nicola and J. R. Pelaez, Phys. Rev. D **65**, 054009 (2002), hep-ph/0109056.